Available online at www.sciencedirect.com
ScienceDirect
Catalysis Today 127 (2007) 256–264
CATALYSIS TODAY
www.elsevier.com/locate/cattod

Steam reforming of the aqueous fraction of bio-oil over structured Ru/MgO/Al_2O_3 catalysts

Aristides C. Basagiannis, Xenophon E. Verykios *

Department of Chemical Engineering, University of Patras, GR-26500 Patras, Greece

Available online 23 April 2007

Abstract

A catalyst consisting of Ru (5%) dispersed on 15% MgO/Al_2O_3 carrier exhibits high activity and selectivity, as well as satisfactory stability with time on stream, under conditions of steam reforming of acetic acid, a model compound for pyrolysis oil. The presence of MgO in the catalyst formulation is shown to be related to oxygen and/or hydroxyl radical spillover from the carrier to the metal particles. A series of Ru/MgO/Al_2O_3 catalysts supported on cordierite monoliths, ceramic foams and γ-Al_2O_3 pellets were prepared and tested for the production of hydrogen by catalytic steam reforming of the aqueous fraction of bio-oil. All different structural forms of the catalyst exhibited satisfactory activity, converting completely the bio-oil, good selectivity toward hydrogen and satisfactory stability with time on stream. However, the catalyst supported on pellets exhibited the best catalytic performance, among all catalysts investigated. Reforming reactions, and thus hydrogen production, are favoured at high temperatures and low space velocities. Coking is one of the most significant problems encountered in these processes. It was found that only a small part of the incoming carbon is deposited on the catalyst surface, which is mainly present as CH_x. However, coke deposition is more intense on the reactor wall above the catalytic bed, due to homogeneous polymerization of unstable ingredients of bio-oil.

Keywords: Pyrolysis oil; Steam reforming; Ruthenium catalysts; Hydrogen production

1. Introduction

Interest towards the utilization of renewable energy sources is constantly increasing, in view of growing environmental concerns, such as global warming, and concerns over the projected depletion of fossil fuel reserves. Hydrogen, in combination with fuel cells, is being considered as an environmentally friendly source of energy for automotive as well as stationary applications. Fuel cells provide higher efficiency in energy production, as compared to other electric power generating systems. At present, there are many well-established processes for hydrogen production from fossil fuels, such as naptha, natural gas and coal [1]. However, real environmental benefits are linked to the ability to produce hydrogen from renewable sources with no net production of greenhouse gasses. Renewable hydrogen can be produced from biomass by several approaches, such as biomass gasification [2] or steam reforming of bio-fuels, such as bio-ethanol [3–6].

The bio-oil (or pyrolysis oil) derived from fast pyrolysis of biomass represents another potential source of renewable hydrogen and other valuable chemicals. Fast pyrolysis has made significant advances over the past 20 years [7]. It requires rapid heating of biomass particles at temperatures of about 500 °C and short residence times (0.5–1 s), so as to decompose, generating vapors, aerosols and charcoal [8]. Under such conditions, the yield of the liquid product, pyrolysis oil, can reach 75–80 wt% [9]. The composition of pyrolysis-oil varies significantly with the type of biomass and the conditions of pyrolysis. However, elemental analysis of pyrolysis-oil derived from different processes shows that its main components include the following groups: acids, alcohols, aldehydes, esters, ketones, sugars and phenols [10].

Steam reforming of pyrolysis-oil can be described by the following reaction stoichiometry:

$$C_nH_mO_k + (n-k)H_2O \rightarrow nCO + \left(n + \frac{m}{2} - k\right)H_2 \quad (1)$$

This reaction is followed by the water gas shift (WGS) reaction:

$$CO + H_2O \leftrightarrow CO_2 + H_2 \quad (2)$$

* Corresponding author. Tel.: +30 2610 991527; fax: +30 2610 991527.
E-mail address: verykios@chemeng.upatras.gr (X.E. Verykios).

0920-5861/$ – see front matter © 2007 Elsevier B.V. All rights reserved.
doi:10.1016/j.cattod.2007.03.025

Thus the overall process (complete steam reforming of pyrolysis-oil) can be represented as follows:

$$C_nH_mO_k + (2n-k)H_2O \rightarrow nCO_2 + \left(2n + \frac{m}{2} - k\right)H_2 \quad (3)$$

Steam reforming of pyrolysis oil (Eq. (3)) is an endothermic reaction, favoured at high temperatures.

Experimental investigations of this reaction present significant difficulties, especially with respect to carbonaceous deposits (i.e. carbon formation) on the catalyst surface [11,12]. An operational difficulty is related to feeding of the pyrolysis-oil into a laboratory microreactor. Bio-oil cannot be totally vaporized; significant amounts of residual solids are formed when it is heated above 90 °C due to polymerization reactions of various components. For this reason, the most appropriate way to feed the oil into the reactor is by spraying, using a nozzle injection system. Of course, the single use of an injection system does not solve problems with undesirable reactions. Due to these objectively significant difficulties, studies dealing with the reformation of pyrolysis-oil itself are rare. Recently, Rioche et al. [13] reported for the first time a study dealing with the reaction of steam reforming of pyrolysis-oil over noble metal catalysts. However, these workers did not use a high-pressure nozzle injection system but, instead, they fed pyrolysis-oil using a syringe pump (droplet by droplet).

Studies dealing with model compounds of bio-oil, such as acetic acid, are more frequent in the literature and describe promising results [14–17]. Reports describing the reformation of the aqueous fraction of bio-oil have been published by Chornet and co-workers [18,19]. This group is the first which has dealt with the process of steam reforming of bio-oil, and they have also proposed an integrated process concept of hydrogen production via bio-oil [20]. They have mainly tested commercial or Ni-based catalysts. However, they have not used the entire bio-oil, but only its aqueous fraction or model compounds. Recently, another report dealing with the reformation of the aqueous fraction of bio-oil has been published [21].

In our previous communications [22–24], the catalytic performance of various supported metal catalysts under conditions of steam reforming of acetic acid, a model compound of bio-oil, was discussed. It was found that Ni-based and Ru-based catalysts offer the best catalytic performance. Also, the reaction network under conditions of steam reforming of acetic acid was investigated over these catalysts [22,24]. The 5% Ru/MgO/Al_2O_3 catalyst was found to be the most promising one, presenting the highest activity and hydrogen selectivity, as well as very stable performance with time on stream.

Aim of the present work is to test this catalyst under more realistic conditions, i.e. using the aqueous fraction of bio-oil as reactant. The Ru catalyst was prepared in structured forms (i.e. pellets, ceramic monolith and ceramic foam) and the liquid was fed into the reactor by spraying, using a nozzle.

2. Experimental techniques

2.1. Catalysts preparation

A series of 5% Ru/(15% MgO/Al_2O_3) catalysts were supported on cordierite monoliths, ceramic foams and pellets. Two different kinds of cordierite monoliths were used: one with 400 channels and a second one with 1200 channels per square inch. The ceramic foams were proprietary formulations of alumina and zirconia with medium porosity (50 pores per square inch). The pellets were 1/16 in. extrudates of γ-Al_2O_3 (Engelhard) with a specific surface area of 148.2 m^2/g.

The MgO/Al_2O_3 support was synthesized by impregnating γ-Al_2O_3 pellets with $Mg(NO_3)_2$ (Alfa Aesar), as Mg precursor, followed by drying at 110 °C overnight, and calcination at 900 °C for 16 h. The MgO content on Al_2O_3 was invariant 15 wt%. The Ru/MgO/Al_2O_3 catalyst was prepared by the wet impregnation method using $Ru(NO)(NO_3)_3$ as Ru precursor, followed by drying at 110 °C overnight, and calcination at 300 °C for 2 h. The nominal Ru loading was invariantly 5 wt%. A powder of the same catalyst was also prepared with the same technique. However, this catalyst was ground and sieved, in order to achieve very small particle size, smaller than 63 μm. A dense suspension of this catalyst powder in de-ionized water was created and the monoliths were coated by successive immersions in the suspension followed by overnight drying at 110 °C and calcination at 500 °C. A final calcination at 900 °C took place before testing. A total of 1.85 g of catalyst was loaded on a monolith 24 mm in diameter, 40 mm in length and weighing 6.6 g (loading 1.7 g/in.^{3}).

A second monolith, having the same dimensions as the previous one, but with 1200 channel per square inch, was supplied by Johnson Matthey (JM). This catalyst was coated with the same catalyst, using the same technique and achieved a loading of 2.2 g/in.^{3} (2.4 g of the catalyst were loaded on the monolith). Also, a ceramic foam coated with the same catalyst was supplied by JM. The foam had a diameter of 25 mm and length of 24 mm, while the catalyst loading was 2.9 g/in.^{3} (2 g of the Ru catalyst were loaded on the foam).

2.2. Apparatus and experimental procedure

Catalytic performance experiments were carried out using an apparatus which consists of a flow system, the reactor unit and the analysis system. The flow system is consisted of four mass flow controllers (MKS Instruments) for the regulation and control of gas flows. Feeding of the liquid (aqueous fraction of bio-oil) into the reactor was achieved by using an HPLC pump (Marathon, Scientific Systems) and a nozzle injection system. The analysis system consists of two gas chromatographs (GC 14A and GC-8B, Shimadzu). The specific apparatus, apart from the reactor, is described in detail in a previous communication [23].

As mentioned previously, feeding of the liquid into the reactor was achieved using a nozzle. However, a nozzle with the desirable flow rate could not be found. To overcome this difficulty, an appropriate reactor was designed and fabricated

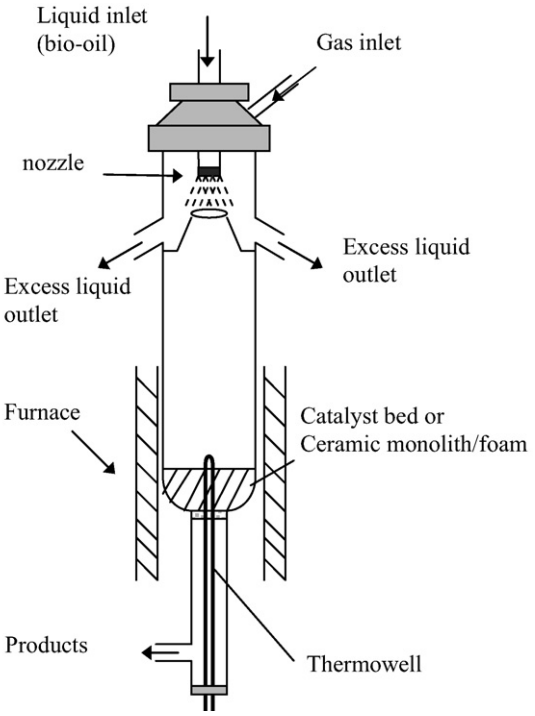

Fig. 1. Schematic diagram of the nozzle-fed reactor employed for the catalytic experiments with the aqueous fraction of bio-oil.

which permitted use of commercially available high flow rate nozzles. A schematic diagram of the nozzle-fed reactor is shown in Fig. 1. The nozzle is attached to the reactor, with proper sealing on the upper side, at a significant distance from the catalyst bed, so as to be maintained at low temperature. A few centimeter below the nozzle, a quartz cone is adapted to the quartz wall. A fraction of the sprayed liquid is collected in the space between the cone and the reactor wall and it is removed via two openings, as shown in the figure. This part of the reactor is out of the furnace, while the rest is in the furnace. The cone has a diameter of about 14 mm and the liquid which passes through it is rapidly directed to the catalyst bed. The rest of the liquid (the larger part) is removed via the by-pass outlets. By changing the distance between the nozzle and the cone, the flow that passes into the reactor can be controlled. The mass of liquid collected in the by-pass section is measured with respect to time. A constant flow of the by-pass liquid with respect to time was determined. The temperature profile of the catalyst bed (or monolith or foam) was measured by a K-type thermo well, which was able to run through the bed.

In a typical experiment, the fresh catalyst is placed in the reactor and reduced in situ at 750 °C for 2 h under pure hydrogen flow. After reduction, the reactor is heated under He flow. At this time, the reactant (aqueous fraction of bio-oil) is introduced into the reactor. Of course, the reactor temperature is decreased due to the introduction of liquid flow. When the system equilibrates at the desired temperature, the conversion of the reactants and selectivities towards reaction products are determined using the analysis system described above.

Calculation of selectivities of reaction products which contain carbon (in the form of C_xH_y or $C_xH_yO_z$) is based on the carbon balance, taking into account the carbon contained in each product and the total amount of carbon produced. Obviously, the sum of these selectivities is 100%. Selectivity towards hydrogen production (S_{H_2}) is based on the amount of hydrogen missing due to the production of hydrogen-containing by-products ($S_{H_2} = 100 - 2 \times S_{CH_4} - 2 \times S_{C_2H_4} - 3 \times S_{C_2H_6} - \ldots$).

Table 1
Composition and physical properties of beech wood oil used in the present study [23]

Elemental composition (%)	
C	38.7
O	53.4
H	7.5
N	0.38
Physical properties	
Water content (wt%)	28.8
Viscosity at 20 °C (cSt)	45.1
Density at 20 °C (g/cm^3)	1.16
pH	3.3

2.3. Bio-oil characteristics

The bio-oil used was produced by fast pyrolysis of beech wood and was supplied by the University of Twente. The average composition of this bio-oil was $CH_{2.3}O_{1.04}N_{0.01}$, including water. The typical moisture content of the oil was 29 wt%. Bio-oil was supplied filtered, in order to remove char particles. Table 1 lists some physical and chemical properties of the bio-oil used [25].

The aqueous fraction of bio-oil was prepared by addition of water in oil. The mass ratio of H_2O/oil was equal to 2. The water solubility of the oil is about 75 wt%, while the solubility of organic compounds is about 60% [25]. This means that the amount of carbon present in the aqueous fraction of bio-oil is about 60% of the initial amount of carbon contained in the entire oil. This results in a steam-to-carbon ratio in the feed equal to 7.2.

3. Results and discussion

3.1. Steam reforming of model compound

The intrinsic catalytic activity as well as stability of the Ru/MgO/Al_2O_3 catalyst, in powder form, is illustrated here using steam reforming of acetic acid. Acetic acid (HAc) is considered to be a model compound of bio-oil, since its content in the oil mixture is relatively high. Results of HAc conversion and product distribution as a function of reaction temperature over the Ru/MgO/Al_2O_3 catalyst under HAc steam reforming conditions are presented in Fig. 2. Conversion of HAc as well as selectivity towards hydrogen production are maintained at the 100% level at temperatures higher than 700 °C. CO and CO_2 are the only other products, implying that the reaction of steam reforming of HAc (Eq. (4)) along with the WGS reaction (Eq. (2)) are the two reactions which take place within this temperature range.

$$CH_3COOH + 2H_2O \rightarrow 2CO_2 + 4H_2 \quad (4)$$

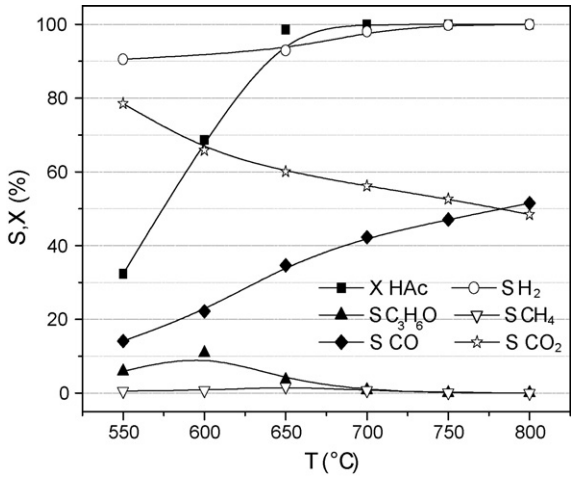

Fig. 2. HAc conversion and product distribution under steady-state conditions over 5% Ru/MgO/Al_2O_3 catalyst. Experimental conditions: mass of catalyst: 100 mg; particle size: 0.18–0.25 mm; H_2O/HAc molar ratio: 3; flow rate: 290 cm^3/min; feed: 7.5% HAc, 22.7% H_2O in He; P = 1 atm.

As reaction temperature decreases, HAc conversion is reduced, and it drops to approximately 70% at 600 °C. Selectivity towards CO production is favoured at higher temperatures, while selectivity toward CO_2 at lower temperatures, as per the equilibrium limitations of the WGS reaction. At temperatures lower than 650 °C hydrogen selectivity is reduced due to the formation of by-products, such as acetone and trace amounts of methane. Acetone is produced probably via the ketonization reaction:

$$2CH_3COOH \rightarrow (CH_3)_2CO + CO_2 + H_2O \quad (5)$$

The long-term stability test with time on stream over the Ru/MgO/Al_2O_3 catalyst is shown in Fig. 3. This catalyst showed very stable catalytic performance for 35 h on stream. During this period of time no by-product is observed, while selectivities of the observed products, H_2, CO and CO_2, are very close to those defined by thermodynamic equilibrium under the present conditions. As conversion of HAc and selectivity towards hydrogen remained at 100%, the total reactant flow rate was increased from 290 to 470 cm^3/min in order to reduce the HAc conversion and record any fluctuation in catalyst performance. The conversion of acetic acid slightly dropped within the next 30 h on stream, but remained stable at about 90%, while selectivity towards hydrogen production remained at very high levels, almost 100%. Selectivity towards CO and CO_2 were stabilized at 40% and 60%, respectively, while the only by-product which was detected was methane, but in very small concentrations ($S_{CH_4} < 2\%$). The stable performance can be attributed to the very low carbon deposition rate over this catalyst [23].

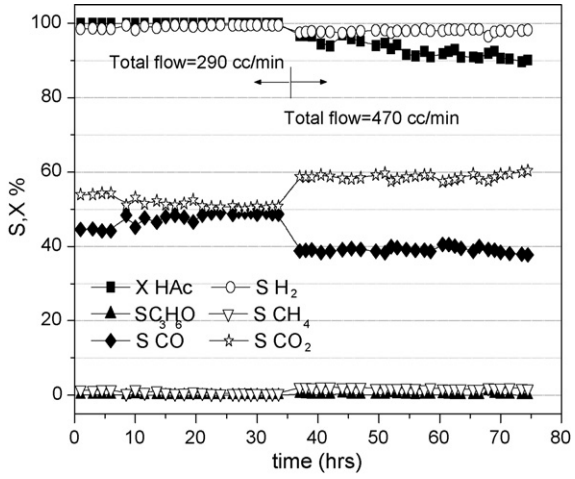

Fig. 3. HAc conversion and product distribution as a function of time on stream over 5% Ru/MgO/Al_2O_3 catalyst. Experimental conditions: mass of catalyst: 100 mg; particle size: 0.18–0.25 mm; H_2O/HAc molar ratio: 3; flow rate: 290 cm^3/min; feed: 24% HAc, 72% H_2O in He, T = 800 °C, P = 1 atm.

3.2. Steam reforming of the aqueous fraction of bio-oil

In the experiments described in the present section, the aqueous fraction of bio-oil was used as reactant. Taking into account the elemental analysis of bio-oil, its water solubility, as well as the solubility of organic compounds (Section 2.3), it was estimated that the ratio of steam-to-carbon (S/C) in the aqueous solution of bio-oil was equal to 7.2. This ratio is fairly high, thus no additional water was added to the feed mixture. This mixture was introduced into the reactor by a nozzle, as described in the Section 2.

The catalytic performance of the structured catalysts was examined as function of reaction temperature, total flow rate (space velocity, W/F ratio), and time on stream (stability). Typical results obtained over the 5% Ru/MgO/Al_2O_3 catalysts in pellet form will first be presented, and then the performance of the different structural forms will be compared. It must be noted that under the present experimental conditions the conversion of bio-oil was complete in all cases.

3.2.1. Influence of operating parameters

The effect of reaction temperature on catalytic performance of the Ru/MgO/Al_2O_3 catalyst in pellet form is shown in Fig. 4, in which selectivities toward reaction products are shown as

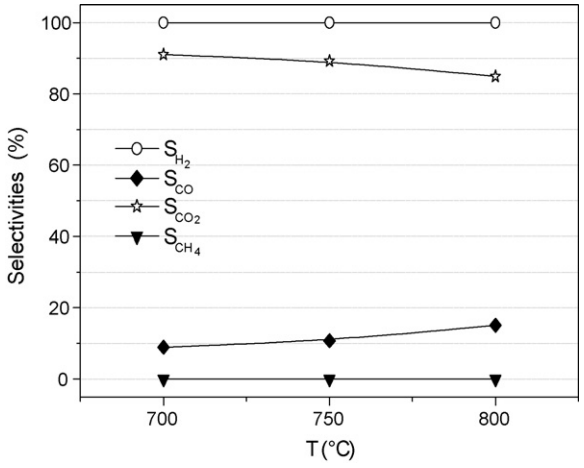

Fig. 4. Product distribution as a function of reaction temperature over the 5% Ru/MgO/Al_2O_3 catalyst in pellet form, under conditions of steam reforming of the aqueous fraction of bio-oil. Experimental conditions: mass of catalyst: 6 g, total flow: 1050 cm^3/min (200 cm^3/min He + a.f. of bio-oil), S/C = 7.2, GHSV = 5200 h^{-1}, P = 1 atm.

function of reaction temperature. Under the specific experimental conditions, the only products which were detected are H_2, CO and CO_2. No by-products are observed. As mentioned above, the conversion of bio-oil is complete, while selectivity towards H_2 production is 100% over the entire temperature range investigated. Selectivity toward CO_2 production is reduced, while that of CO is increased, as temperature increases, due to thermodynamic limitations of the WGS reaction. The observed behaviour of CO_2 and CO selectivities is due to the large S/C ratio (large excess of steam), which shifts the equilibrium toward CO_2 formation. Estimation of the expected WGS equilibrium concentrations under the present conditions reveals that equilibrium is achieved.

The axial temperature profile through the catalyst bed was determined to be nearly flat. Apparently, the endothermicity of the reforming reaction was successfully balanced by rapid heat transport from the furnace. A number of other factors also contribute to that, such as the occurrence of the exothermic WGS reaction, as well as the large excess of water in the feed.

The effect of space velocity on catalytic performance was investigated over the same catalyst and the results are summarized in Fig. 5. The feed composition was maintained constant as described above, while temperature at the entrance of the catalyst bed was also maintained constant, at 800 °C. Space velocity was varied from 4880 to 16,570 h^{-1}. In all experiments, complete conversion of bio-oil was observed. At low flow rates (small GHSV) no by-products are formed. Hydrogen selectivity is 100%, while CO_2 and CO selectivities are about 90 and 10%, respectively, as per the equilibrium of the WGS reaction. At higher flow rates (GHSV = 16,570 h^{-1}), formation of by-products, such as methane and ethylene, is observed, resulting in reduction of hydrogen selectivity. Apparently, reformation of reaction intermediates, such as ethylene and methane, is less rapid than reformation of bio-oil over this catalyst, requiring larger contact times for its completion. It is also observed that selectivity toward CO production is increased, while that of CO_2 is reduced at higher GHSV, implying that the WGS reaction is not achieving equilibrium conditions at very small residence times.

3.2.2. Comparison of the performance of different structured form

In addition to the pellets discussed above, the Ru/MgO/Al_2O_3 catalyst was also supported on a ceramic foam made from zirconia-alumina and on two cordierite monoliths. In this section, a comparison of the catalytic performance of the different structured forms of the catalyst is presented. In these experiments, the feed composition remained the same as described above, while the temperature at the inlet of catalyst bed was maintained at 800 °C. Because of the different amount of active phase in each form, the *W/F* ratio was different at the same flow rate. The term "*W/F*" is the ratio of the weight of the catalyst to the total flow of reactants fed into the reactor. Flow limitations of the apparatus did not allow scanning large envelopes of *W/F* ratios and space velocities for all samples.

As mentioned above, all catalyst forms are able to convert bio-oil completely. The comparison of the different catalysts is based on selectivities of reaction products. Selectivity toward hydrogen production as a function of *W/F* ratio over the four

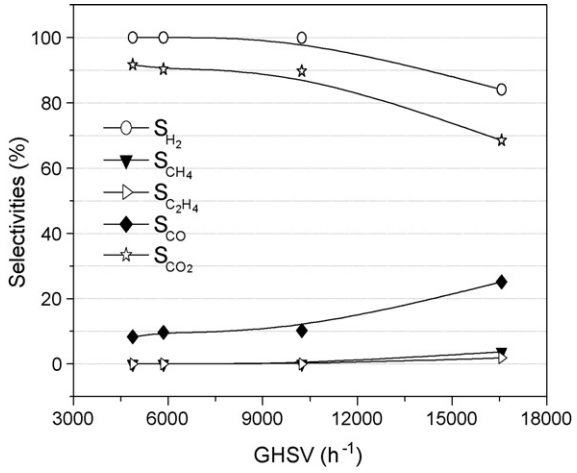

Fig. 5. Product distribution as a function of space velocity over the 5% Ru/MgO/Al_2O_3 catalyst in pellet form, under conditions of steam reforming of the aqueous fraction of bio-oil. Experimental conditions: mass of catalyst: 6 g, *T* = 800 °C, S/C = 7.2, *P* = 1 atm.

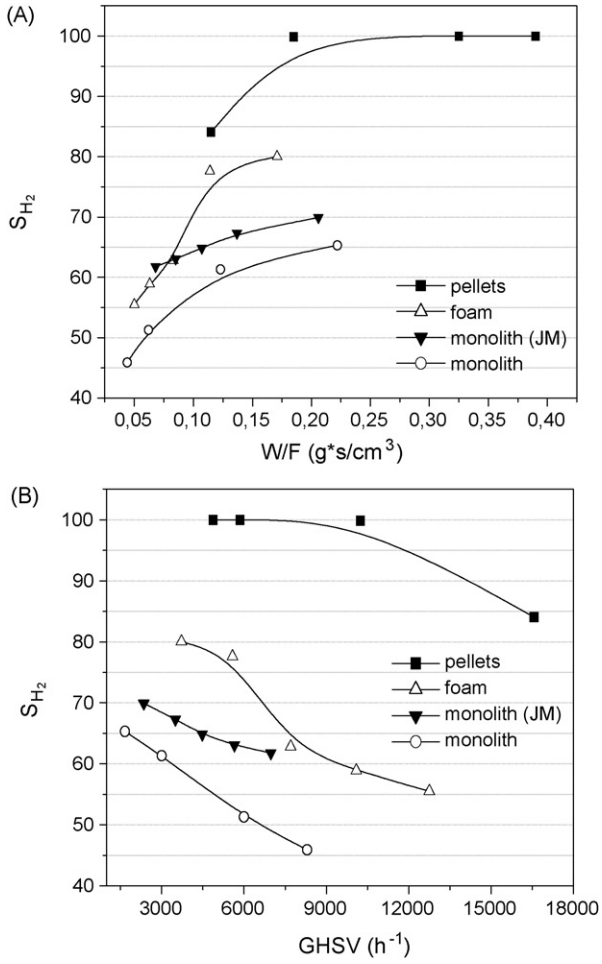

Fig. 6. Comparison of catalytic performance of different structural forms of the catalyst: selectivity toward hydrogen production as a function of *W/F* ratio (A) and space velocity (B). Experimental conditions: S/C = 7.2, *T* = 800 °C, *P* = 1 atm.

different types of Ru catalyst is shown in Fig. 6A. It is apparent, that the highest hydrogen selectivity is exhibited by the Ru/MgO/Al_2O_3 catalyst in pellet form. At high *W/F* ratios (>0.2 g s/cm^3) hydrogen selectivity is maintained at the 100% level, while it is reduced at lower values of *W/F*. This implies that reforming reactions are not complete at very large flow rates or relatively short contact times. The ruthenium catalyst supported on the ceramic foam exhibits lower values of hydrogen selectivity as compared to the pellets, while the two coated monoliths exhibit the lowest selectivity toward hydrogen production under all experimental conditions. Hydrogen selectivity as a function of space velocity is shown in Fig. 6B. The relative rank of the four catalysts remains also the same, indicating that a reactor operating with pellets is more efficient than a reactor operating with ceramic foam or monolith, both on a volume basis as well as a mass of catalyst basis.

Carbon oxides are primary products of reforming reactions and selectivities towards CO and CO_2 production may reflect the ability of the catalyst to promote the WGS reaction. CO_2 and CO selectivities as functions of *W/F* ratio are shown in Fig. 7A and B, respectively. The catalyst in pellet form presents the largest CO_2 selectivity and the lowest selectivity towards CO, implying that this catalyst is very active in promotion of the WGS reaction. The coated foam exhibits lower CO_2 selectivity than the pellets, while over the two monoliths the CO_2 production is the lowest among all catalysts investigated. Of course, the trend of the selectivity towards CO production (Fig. 7B) follows exactly the inverse mode compared to that of CO_2, due to WGS limitations.

The main by-products observed are methane and, in some cases, ethylene. Selectivities of the different catalysts toward CH_4 formation, shown in Fig. 7C, are inversely proportional to those shown for hydrogen (Fig. 6). The ruthenium catalyst in pellet form exhibits the lowest values of CH_4 selectivity. Over the other catalysts, methane production is much higher, implying that reforming reactions are not complete under these conditions. In certain cases, ethylene is also observed in the reformate gas, but in much lower concentrations. Ethylene selectivity is nearly zero for low flow rates, and it increases at higher flow rates (Fig. 7D).

The selectivity toward hydrogen and the selectivity toward CO_2 reflect, to a large extent, the activity characteristics of the different structural forms of the catalyst toward reforming reaction and toward the WGS reaction. Of course, the different structural forms also affect mass transfer characteristics within the system, which contribute to the alteration of catalytic activity and selectivity. The reformation of the oil components and intermediates leads to hydrogen formation. When the activity is high, no intermediates, such as CH_4 or C_2H_4, are observed. However, when the activity is not high enough, such reactions intermediates survive in the gas phase. This implies

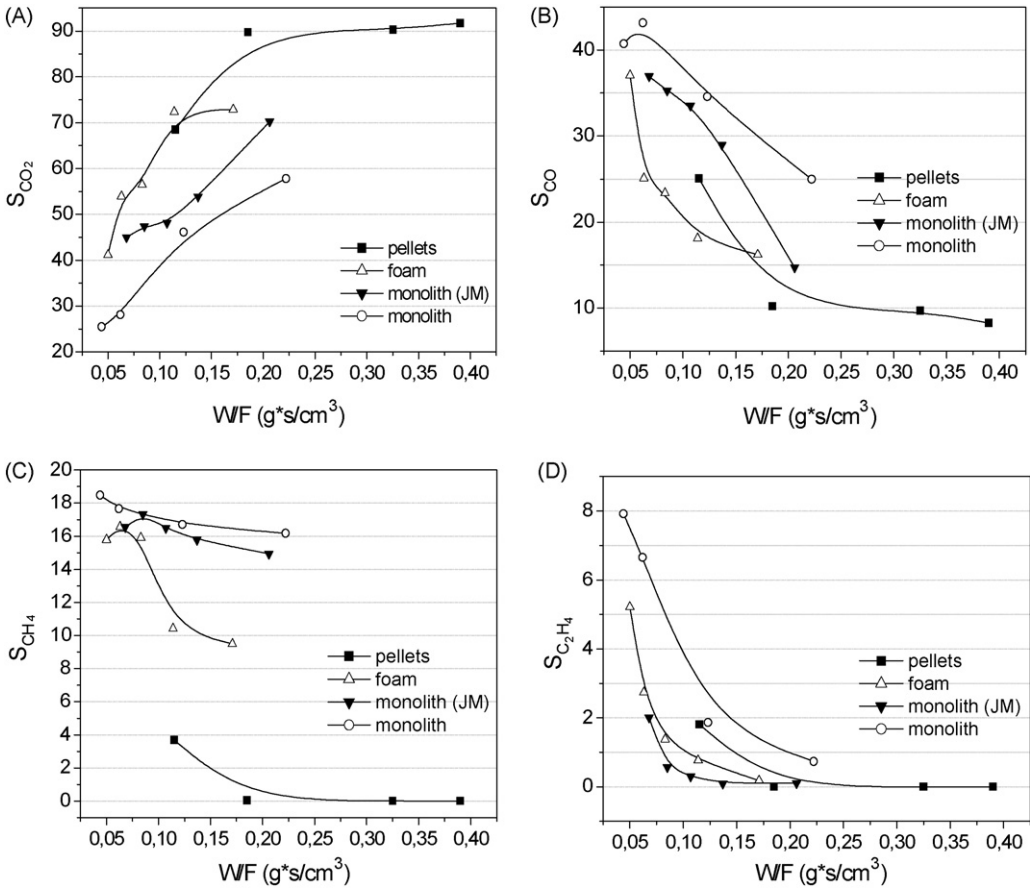

Fig. 7. Comparison of catalytic performance of different structural forms of the catalyst: selectivity toward CO_2 (A), CO (B), CH_4 (C) and C_2H_4 (D) production, as a function of *W/F* ratio. Experimental conditions: same as in Fig. 6.

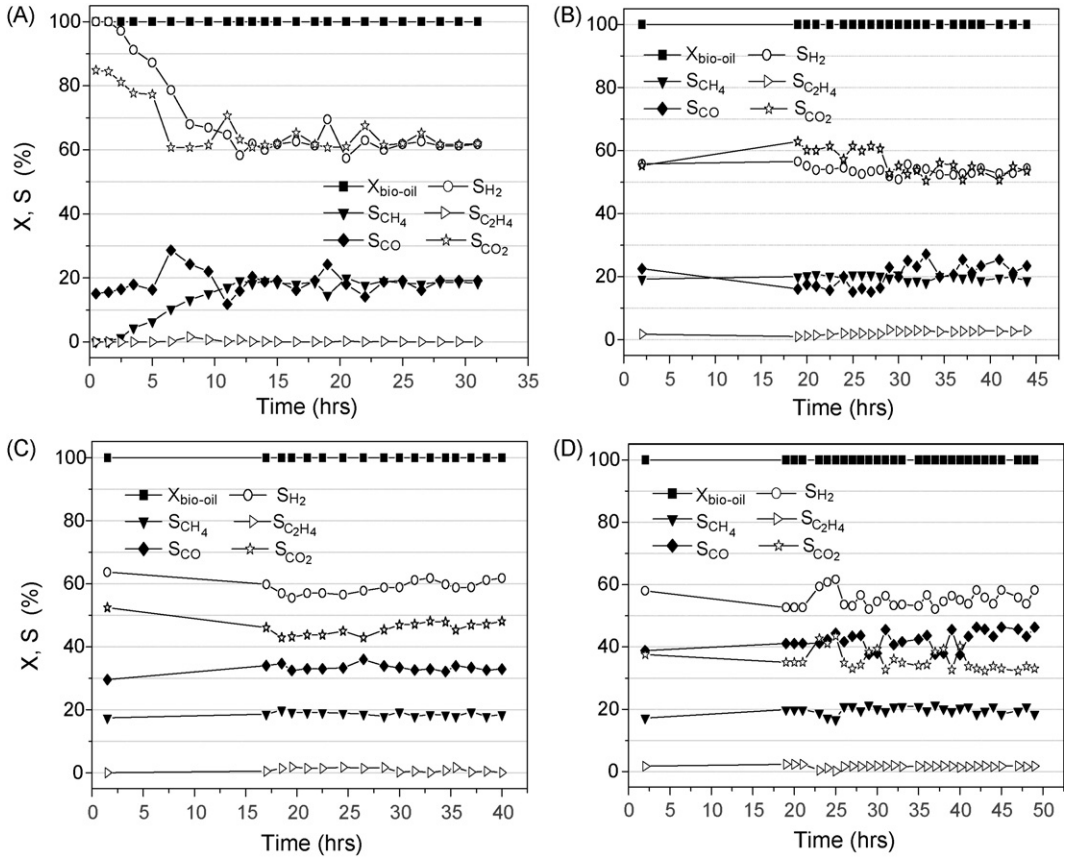

Fig. 8. Long-term stability test over 5% $Ru/MgO/Al_2O_3$ catalyst in pellet form (A), ceramic foam (B), ceramic monolith JM (C) and ceramic monolith (D). Experimental conditions: $T = 700\ ^\circ C$, GHSV = 5900 h^{-1} (A), $T = 800\ ^\circ C$, GHSV = 7200 h^{-1} (B), $T = 800\ ^\circ C$, GHSV = 4200 h^{-1} (C) and $T = 800\ ^\circ C$, GHSV = 4350 h^{-1} (D), S/C = 7.2, $P = 1$ atm.

that a series reaction is taking place: decomposition/reformation of the pyrolysis oil components into various intermediates, followed by further reaction toward carbon oxides and hydrogen. The reformation of certain intermediates – such as methane and ethylene – is slow as compared to the initial reaction.

3.2.3. Catalyst stability

The four different types of structured ruthenium catalysts were also tested for their stability with time on stream and the results are shown in Fig. 8A–D. In the case of pelleted catalyst (Fig. 8A), selectivities toward H_2 and CO_2 production are initially very high and are gradually reduced during the first 10 h of operation. Methane selectivity is initially rather low and is gradually increased, following the inverse behaviour of hydrogen selectivity since they are the only hydrogen-containing products of the reaction which were detected. Product distribution remains stable for more than 25 h. The main products during stable operation are H_2, CO, CO_2 and CH_4 of which selectivities are stabilized at the level of 60, 20, 60 and 20%, respectively. However, the conversion of bio-oil remains complete during the entire experiment.

The performance of the other three structured catalysts is similar to that of the pellets. Their corresponding stability tests are presented in Fig. 8B–D. Again, the main products detected in the reformate gas are H_2, CO, CO_2 and CH_4. Over the coated foam, the selectivities of main products are similar to those in the case of pellets (Fig. 8B), while over the coated monoliths (Fig. 8C and D) selectivity toward CO is higher, at the expense of CO_2, as compared to the pellet form of the catalyst. All structural forms, however, exhibit good stability with time on stream, over a 40–50 h operation.

3.2.4. Estimation of the rate of carbon deposition under reaction conditions

Carbon deposition is one of the most significant problems in reforming processes, which usually results in gradual deactivation of the catalyst. In the present study, the amount of carbon deposited on the catalytic surface during the long-term stability experiments was estimated and characterized by isothermal combustion and by Temperature Programmed Oxidation (TPO) techniques. In the former case, the coked catalysts were exposed to flow (40 cm^3/min) of a 3% O_2/He mixture at the temperature of 750 °C, for the estimation of the total amount of carbon deposited on their surface. In the later case, TPO with 1% O_2/He was performed for spent catalytic samples, in order to characterize the carbonaceous deposits. In both cases CO_2 was the only product detected and its evolution was followed and quantified by mass spectrometer.

Integration of the CO_2 curves produced during the combustion at 750 °C showed that only a small fraction of incoming carbon is deposited on the catalytic surface (0.05–

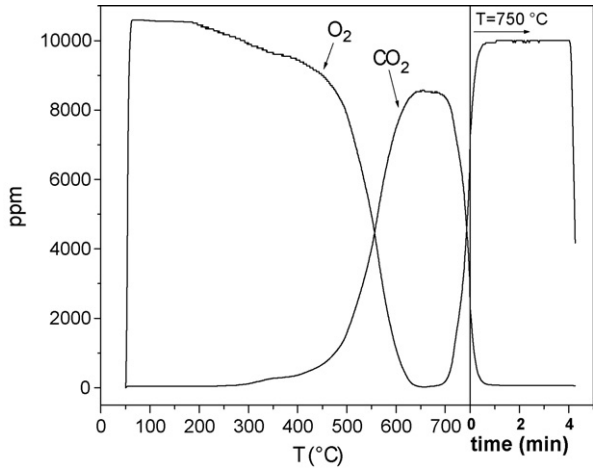

Fig. 9. O_2 and CO_2 responses of TPO of carbon deposited on a sample of spent Ru monolith (JM) catalyst. Experimental conditions: total flow: 40 cm^3/min, feed: 1% O_2/He, $\beta = 15$ °C/min.

0.11%). Formation of carbonaceous deposits is more intense on the reactor wall above the catalytic bed, due to homogeneous polymerization of bio-oil components. This amounts to about 8 wt% of the incoming carbon. However, this amount is much smaller than that which other researchers have reported (∼30 wt%), for steam reforming of the aqueous fraction of bio-oil under similar conditions [21]. This may be due to the fact that in the present work the liquid is fed into the reactor by spraying, which results in minimization of carbon deposits. This then may imply that a more meticulous design of the reactor (i.e. spraying angle, reactor dimensions, distance between nozle and catalyst) could result in further reduction of the homogenously produced carbon.

The TPO spectrum obtained over a sample of the spent monolith (JM) is presented in Fig. 9. CO_2 was the only product detected and its production is initiated at about 300 °C, while the largest part of coke is burned at temperatures higher than 500 °C. Carbon dioxide production exhibits a broad maximum at about 630 °C, indicating that this temperature is adequate to remove coke deposited on the catalytic surface. To further elucidate the nature of carbon deposits, especially their chemical composition (CH_xO_y), material balances of oxygen consumed and CO_2 formed were performed. The amount of O_2 which was consumed was found to be higher than that corresponding to produced CO_2, presenting a deviation of ∼15%. This observation implies that the carbonaceous deposits which are present on the catalyst surface are of the CH_x form, in agreement with the results of Kechagiopoulos et al. [21].

3.3. The role of MgO in Ru/MgO/Al_2O_3 catalyst

The 5% Ru/MgO/Al_2O_3 catalyst, in all structural forms investigated, seems to be very active and selective, as well as sufficiently stable with time on stream, under conditions of steam reforming of the aqueous fraction of bio-oil. To the best of our knowledge, no other catalysts have been tested for stability under conditions of steam reforming of bio-oil, for extended time periods. Rioche et al. [13] tested a Pt/$CeZrO_2$ catalyst for a total period of time on stream of 9 h under a liquids (bio-oil + water) flow of 56 μL/min. The good stability of the Ru/MgO/Al_2O_3 catalyst can be attributed to the high activity of ruthenium in reforming reactions, as well as the presence of the MgO/Al_2O_3 support, which is in the magnesium aluminate spinel form [24]. Magnesium aluminate spinel is considered to be more stable toward sintering than alumina itself [26,27]. Also, it has been shown [28] that magnesium oxide may contribute to the stabilization of the metal particles at high temperatures under steam, thus preventing their sintering. However, these characteristics of MgO/Al_2O_3 support are related more with the stability rather than with the high activity of the Ru/MgO/Al_2O_3 catalyst.

The enhanced steam reforming activity of the Ru/MgO/Al_2O_3 catalyst, as compared to the Ru/Al_2O_3 catalyst, and the role of MgO in the catalytic process should be assessed with respect to mechanistic aspects of the catalytic system. It has been proposed [18,29] that the reaction mechanism of steam reforming of oxygenates consists of two important reaction pathways. In the first one, the oxygenate is primarily dissociated on the metal leading to adsorbed hydrocarbon fragments. In the second pathway, steam adsorption and dissociation occur mainly on the support surface. The resulting –OH groups migrate onto the metal particles through the metal/support interface. Once on the metal, they react rapidly with hydrocarbon fragments and various intermediates to give CO, CO_2 and H_2. The ability of the catalytic system to keep the metal surface clean through O and –OH spillover processes seems to be an important step toward catalytic activity and stability.

The spillover process of O and –OH groups over the Ru/MgO/Al_2O_3 catalyst was investigated in the present study, in an indirect manner, by conducting temperature programmed reduction (TPR) experiments using CO as a reactant. Such experiments were conducted over the Ru/MgO/Al_2O_3 and the Ru/Al_2O_3 catalysts, and the oxidation of CO – which takes place only on the metal surface – was used to monitor the process of the oxygen and/or hydroxyl anion spillover onto the metal particles. Thus, the role of MgO in the spillover process can be elucidated. Both catalysts were reduced with pure hydrogen flow at 700 °C for 1 h, and then cooled under He flow to room temperature. At this point, 40 cm^3/min of a mixture consisting of 0.25% CO/He was directed into the reactor. The catalyst was kept at room temperature for 10 min, followed by a temperature ramp to 750 °C with a linear rate of 30 °C/min. Evolution of CO and CO_2 in the gas phase was followed by mass spectrometer. The resulting TPR spectra are shown in Fig. 10, where the CO consumed and the CO_2 produced are plotted with respect to temperature, for each catalyst. Since, at the start of the experiment the metal is in its reduced state and the entire surface of the catalyst is free of any adsorbed oxygen, the production of CO_2, which occurs simultaneously with the consumption of CO (Fig. 10), is safely attributed to reaction of CO with O and/or –OH anions which spillover from the support onto the metal surface. It must be stated that (a) the support alone is not capable of oxidizing CO within the temperature range investigated and (b) the Boudouard reaction ($2CO \rightarrow CO_2 + C$) is not taking place in any appreciable

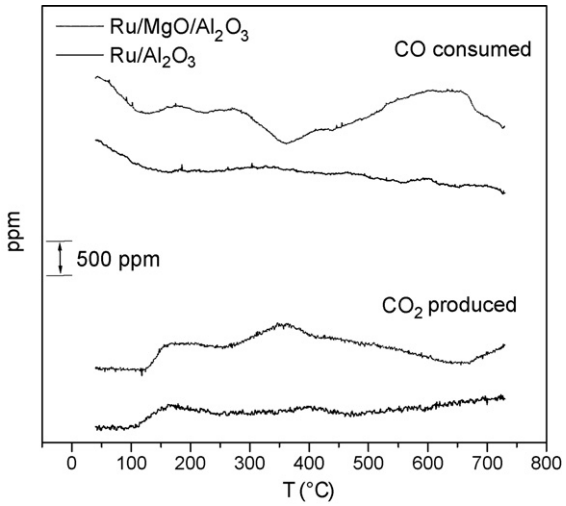

Fig. 10. CO and CO_2 responses of TPR with CO of Ru/Al_2O_3 and $Ru/MgO/Al_2O_3$ catalysts. Experimental conditions: total flow: 40 cm^3/min, feed: 0.25% CO/He, $\beta = 30$ °C/min.

extent since no carbon was detected on the metal surface (by TPO), after completion of the TPR experiments.

It is obvious from Fig. 10 that CO_2 evolution follows closely CO consumption, indicating that CO oxidation is the only source of CO_2 production. Although the total surface area of the two catalysts is nearly the same (81.3 m^2/g for the $Ru/MgO/Al_2O_3$ and 79.0 m^2/g for the Ru/Al_2O_3 catalyst) and the ruthenium dispersion is very close (12.0% for the $Ru/MgO/Al_2O_3$ and 8.8% for the Ru/Al_2O_3 catalyst), the amount of CO_2 produced over the $Ru/MgO/Al_2O_3$ catalyst is significantly higher than the corresponding amount produced over the Ru/Al_2O_3 catalyst. Integration of the curves of Fig. 10 reveals that the amount of CO_2 produced over the $Ru/MgO/Al_2O_3$ catalyst is 1.08 μmol CO_2/m^2 and that over the Ru/Al_2O_3 catalyst 0.57 μmol CO_2/m^2. This difference can be attributed to enhanced spillover of O and/or –OH anions from the carrier surface onto the surface of the metal particles, caused by the presence of MgO and the subsequent transportation of the carrier into magnesium aluminate spinel, as discussed elsewhere [24].

The presence of magnesium is also known to enhance steam adsorption capacity of the catalyst [18]. This factor may also result in improved catalytic activity, since steam adsorption is playing an important role in the mechanism of the reaction of steam reforming, as described above.

4. Summary and conclusions

Based on the results of the present work, it can be concluded that hydrogen production from bio-oil via steam reforming is a feasible process. The 5% $Ru/MgO/Al_2O_3$ catalyst supported on structural materials provides high activity and good selectivity under conditions of steam reforming of the aqueous fraction of bio-oil. It also exhibits good stability with time on stream. Reforming reactions, and thus hydrogen production, are favoured at high temperatures and low space velocities. Highest activity was observed over the catalyst in pelleted form. This is attributed to more efficient contact between the gas phase and the solid phase. Coke formation is more intense on the reactor wall above the catalytic bed due to homogeneous polymerization of unstable ingredients of bio-oil, while only a small percentage of carbon is deposited on the catalyst surface, which is in CH_x form. The role of MgO in the catalyst composition seems to be related to enhanced O and/or –OH anion spillover from the carrier onto the metal particles.

Acknowledgements

This work was funded in part by the Commission of the European Community, under contract ENK5-CT-2002-00634. The authors wish to thank M. Feaviour of Johnson Matthey for supplying certain catalysts samples on request, W. Prins and S. Kersten of the University of Twente for supplying the bio-oil produced by BTG and F. Zimbardi of ENEA for the analysis performed on bio-oil.

References

[1] M.A. Pena, J.P. Gomez, J.L.G. Fierro, Appl. Catal. A 144 (1996) 7.
[2] J. Herguido, J. Corella, J. Gonzalez-Saiz, Ind. Eng. Chem. Res. 31 (1992) 1274.
[3] A.N. Fatsikostas, D.I. Kondarides, X.E. Verykios, Chem. Commun. 9 (2001) 851.
[4] A.N. Fatsikostas, D.I. Kondarides, X.E. Verykios, Catal. Today 75 (2002) 145.
[5] S. Cavallaro, Energy Fuels 14 (2000) 1195.
[6] G.A. Deluga, J.R. Salge, L.D. Schmidt, X.E. Verykios, Science 303 (2004) 993.
[7] D.S. Scott, J. Piskorz, D. Radlein, Ind. Eng. Chem. Process Des. Dev. 24 (1985) 581.
[8] A.V. Bridgwater, J. Anal. Appl. Pyrol. 51 (1999) 3.
[9] A.A. Iordanidis, P.N. Kechagiopoulos, S.S. Voutetakis, A.A. Lemonidou, I.A. Vasalos, Int. J. Hydrogen Energy 31 (2006) 1058.
[10] A. Oasmaa, D. Meier, in: A.V. Bridgwater (Ed.), Fast Pyrolysis of Biomass: A Handbook, vol. 2, CPL Press, Newbury, UK, 2002.
[11] J.R. Rostrup-Nielsen, Catal. Today 37 (1997) 225.
[12] D.L. Trimm, Catal. Today 49 (1999) 3.
[13] C. Rioche, S. Kulkarni, F.C. Meunier, J.P. Breen, R. Burch, Appl. Catal. B 61 (2005) 130.
[14] D. Wang, D. Montane, E. Chornet, Appl. Catal. A 143 (1996) 245.
[15] M. Marquevich, S. Czernik, E. Chornet, D. Montane, Energy Fuels 13 (1999) 1160.
[16] K. Takanabe, K. Aika, K. Seshan, L. Lefferts, J. Catal. 227 (2004) 101.
[17] K. Takanabe, K. Aika, K. Inazu, T. Baba, K. Seshan, L. Lefferts, J. Catal. 243 (2006) 263.
[18] L. Garcia, R. French, S. Czernik, E. Chornet, Appl. Catal. A 201 (2000) 225.
[19] D. Wang, S. Czernik, E. Chornet, Energy Fuels 12 (1998) 19.
[20] S. Czernik, R. French, C. Feik, E. Chornet, Ind. Eng. Chem. Res. 41 (2002) 4209.
[21] P.N. Kechagiopoulos, S.S. Voutetakis, A.A. Lemonidou, I.A. Vasalos, Energy Fuels 20 (2006) 2155.
[22] A.C. Basagiannis, X.E. Verykios, Appl. Catal. A 308 (2006) 182.
[23] A.C. Basagiannis, X.E. Verykios, Int. J. Hydrogen Energy, accepted.
[24] A.C. Basagiannis, X.E. Verykios, in preparation.
[25] F. Zimbardi, C. Freda, F. Nanna, V. Valerio, D. Barisano, Private Communication.
[26] A.D. Mazzoni, M.A. Sainz, A. Caballero, E.F. Aglietti, Mater. Chem. Phys. 78 (2003) 30.
[27] J. Guo, H. Lou, H. Zhao, D. Chai, X. Zheng, Appl. Catal. A 273 (2004) 75.
[28] V.R. Choundary, B.S. Uphade, A.S. Mamman, J. Catal. 172 (1997) 281.
[29] K. Polychronopoulou, J.L.G. Fierro, A.M. Efstathiou, J. Catal. 228 (2004) 417.